Title

Transmission of Progressive Images Over Noisy Channels: An End-to-End Statistical Optimization Framework

Permalink

https://escholarship.org/uc/item/3541n8vn

Journal

IEEE JOURNAL OF SELECTED TOPICS IN SIGNAL PROCESSING, 2(2)

Authors

Yousefi'zadeh, Homayoun
Jafarkhani, Hamid
Etemadi, Farzad

Publication Date

2008-04-01

Peer reviewed

Transmission of Progressive Images Over Noisy Channels: An End-to-End Statistical Optimization Framework

Homayoun Yousefi'zadeh, *Senior Member, IEEE*, Hamid Jafarkhani, *Fellow, IEEE*, and Farzad Etemadi

Abstract—We present a statistical optimization framework for solving the end-to-end problem of multiple antenna transmission of progressive images over noisy channels. Such channels exhibit temporally correlated loss characteristics and are associated with wireless communication links. In our study, we protect the progressive bitstream associated with an image source utilizing a family of rate compatible punctured Reed–Solomon (RS) product codes along with receiver feedback. We consider the impacts of transmission bit errors as well as packet erasures. To cope with the impact of random bit errors, we formulate an optimization problem aimed at minimizing the end-to-end expected distortion of a reconstructed image subject to rate and efficiency constraints. In order to eliminate the impact of packet erasures, we propose utilizing an algorithm that is capable of statistically guaranteeing the delivery of a number of packet sets associated with a progressive bitstream. Our experiments capture the effects of embedding multiple antennas in the transmission of progressive images over wireless tandem channels. Under identical power constraints, our results show that increasing the number of antennas on either transmitting or receiving sides improves the quality of a reconstructed image. Further, the use of receive diversity used in conjunction with simple communication coding schemes such as Maximum Ration Combining (MRC) yields more improvements than the use of transmit diversity used in conjunction with comparable communication coding schemes such as Space–Time Block Code (STBC). Finally, the use of receiver feedback can further improve the quality of an image reconstructed in the absence of feedback.

Index Terms—Multiple antennas, packet erasure, progressive transmission of images, random bit error, temporally correlated loss.

I. INTRODUCTION

PROGRESSIVE image transmission relies on the ability of a source coder to allow a decoder to progressively reconstruct its data at different bit rates from the prefixes of a single bitstream. introduces high sensitivity to transmission noise, i.e., the occurrence of the first error in a set of bits can lead to the loss of progressive property and synchronization as the result of misinterpretation of the remaining bits. Therefore when transmitted over noisy channels, progressive images have to be protected by relying on appropriate channel coding or joint source-channel coding schemes. This paper focuses on the identification of optimal patterns of progressive image transmission over noisy channels.

The work of [17] provides a comprehensive review of the literature material as they pertain to the subject of interest to this paper. In what follows, we review some of the literature articles in the context of progressive source coding and transmission of images. In the area of source coding, the works of [32] introducing embedded zerotrees of wavelets, [30] proposing Set Partitioning In Hierarchical Trees (SPIHT), [25] covering embedded coding of the bitplanes of a wavelet-transformed image, and [20] suggesting yet another progressive wavelet coding technique are perhaps most closely related to our work.

In the area of channel coding and joint source-channel coding, researchers have looked at two closely related but not exactly identical family of problems. These are namely minimizing distortion or distortion-optimal problems and maximizing delivered useful source coding or rate-optimal problems. Rate-optimal problems have been used by many researchers as lower complexity alternatives to distortion-optimal problems. The work of [33] represents an example of solving a rate-optimal problem for a channel with bit errors only. For channels identified by bit errors only, experimental results have shown that the distortion of rate-optimal solutions is not far from the distortion of distortion-optimal approaches for a relatively large class of channel coders.

In [33], the authors proposed concatenating a source coder bitstream with an outer Cyclic Redundancy Check (CRC) coder and an inner Rate Compatible Punctured Convolutional (RCPC) coder. Focusing on the rate-optimal problems and variable-length packets with fixed data payloads, the authors of [10] and [9] proposed the use of dynamic programming and exhaustive search for protecting the source coder bitstream transmitted over Binary Symmetric Channels (BSC) and channels with memory, respectively. They also solved a suboptimal problem with dynamic programming. The authors of [36] provided an algorithm capable of accelerating the computation of the optimal strategy of [10] for the case of fixed-length packets. The authors of [5] proposed the use of a brute-force search algorithm to solve a distortion-optimal problem in a BSC to protect JPEG2000 coded images with an outer CRC coder and an inner punctured turbo coder. The authors of [4] solved the distortion-optimal version of the problem of [10] for fixed size packets in quadratic time. In [27], the authors utilized Low Density Parity Check (LDPC) codes along with a revised version of the algorithm of [5] to transmit JPEG2000 and SPIHT coded images over channels with and

without memory. In [42], the authors used a product code with a turbo coder at the rows to combat bit errors and an RS coder at the columns to compensate against packet erasures. They utilized a two-step iterative optimization approach to identify near-optimal parity assignments of turbo and RS coders. In [3], the exponential rate-distortion model of an image coder was used to analytically solve the distortion-optimal problem for a BSC. In [19], a similar distortion-optimal problem was solved relying on data fitting techniques for BSCs. When attempting at applying their approach to the case of channels with memory, their approach resulted in very conservative estimates of channel error probability. As an alternative to directly applying channel coding techniques in conjunction with the source coding techniques, the authors of [35] proposed utilizing a Maximum *A Posteriori* (MAP) detector to compensate for the impacts of spatially correlated compressed bitstreams as well as temporally correlated channel errors. Their approach called for the utilization of interleaving techniques when dealing with temporally correlated channel errors. Without investigating the optimality of their approach, the authors of [11] showed the potential advantage of using a hybrid technique for adding channel coding to wavelet-based zerotree encoded images and reordering the resulting embedded zerotree bitstream into packets with a small set of wavelet coefficient trees.

Besides the tandem schemes mentioned above, there are also a large set of Channel Optimized Vector Quantization (COVQ) literature articles following the work of [14]. The work of [26] is among such schemes showing relative effectiveness of COVQ in terms of addressing performance-complexity tradeoff in noisy channels with and without memory.

Our review of the literature articles reveals that there is a lack of 1) analysis and quantification of the effects of utilizing multiple antennas when transmitting progressive images over wireless tandem channels and 2) capturing of the effects of utilizing multiple round feedback transmission.

This paper proposes an end-to-end statistical optimization framework for multiple antenna transmission of progressive images over noisy channels. The framework consists of two components applied in the form of a product channel code the combination of which is capable of dealing with temporally correlated random bit errors and packet erasures. The random bit error component is materialized by applying a Reed–Solomon (RS) channel coder for correcting the errors at the row level. A CRC is further used in a serial concatenation with the RS coder for detecting bit errors. We note that the combination of RS+CRC coders can be applied to either a distortion-optimal or a rate-optimal problem. Further, it can be applied to both fixed-length and variable-length packet scenarios. The statistical packet erasure component is materialized by applying an RS coder at the column level. The component further includes an algorithm that can guarantee the delivery of a block of packets formed by a number of symbols with a given probability for both memoryless channels and channels with memory. We note that while the use of a product code introduces further decoding complexity compared to a one dimensional code, its use is justified considering the fact that ignoring either bit errors or packet erasures can yield significant performance degradations in the transmission of multimedia.

Although the framework of this paper may resemble the works of [13], [28], [29], [38], [42] from the standpoint of considering transmission over channels with bit errors and packet erasures, it has to be noted that those articles consider neither the effects of embedding multiple antennas within an optimization problem nor the effects of using feedback for image delivery. Thus, this paper attempts at analyzing and quantifying performance improvements of end-to-end image delivery systems over wireless tandem channels as the result of utilizing multiple antennas as well as multiple round feedback transmissions.

It is also important to emphasize on the fact that the framework of this paper does not represent a case study. While different components have been gathered to form a complete end-to-end transmission system, the framework can transparently work with different alternatives of each component. For example, the use of multiple antennas can be considered in cojunction with other coding schemes such as RCPC codes, turbo codes, and LDPC codes.

This paper is organized in a top-down fashion, i.e., the overall functionality in the form of an integrated protocol is described first. Once an understanding of the system functionality is developed, the individual components are described in further details. Accordingly, the outline of the paper follows. In Section II, we describe our integrated protocol. In Section III, we discuss the details of calculating the symbol error rates of multiple antenna links, our hybrid modeling of the channel loss, and the channel coding technique utilized in our work. In Section IV, we discuss the random bit error component of our optimization framework. The discussion of this section introduces a probabilistic formulation of the optimization problem the cost function of which is derived utilizing the hybrid loss model of Section III. This section, also provides a low complexity solution to the optimization problem. In Section V, we describe the statistical packet erasure component of our framework. In Section VI, we numerically validate our results. Finally, Section VII includes a discussion of concluding remarks and future work.

II. DESCRIPTION OF THE END-TO-END PROTOCOL

In this section, we provide a description of our end-to-end integrated protocol. We consider the transmission of a bitstream produced by a progressive image source coder such as SPIHT [30] or JPEG2000 [41] over a noisy channel. Considering the progressive nature of the source coder, a reconstruction of the transmitted source image can be created from a prefix of the bitstream. The quality of the reconstructed image can be further enhanced by receiving more information in order. We note that due to the progressive nature of transmission, the lack of any number of bits in the final sequence can potentially render subsequently received bits useless. We assume that the bitstream is packetized into a number of packets with a fixed or a variable number of source bits per packet. We consider errors associated with both bit errors and packet erasures. The utilization of error detection and error correction channel codes can potentially compensate for the error effects at both bit and packet levels. Examples of such codes are RCPC codes [16]; punctured turbo codes [1] and [22]; or rate compatible punctured RS codes [43] and [21]. Encoding the information bits of individual
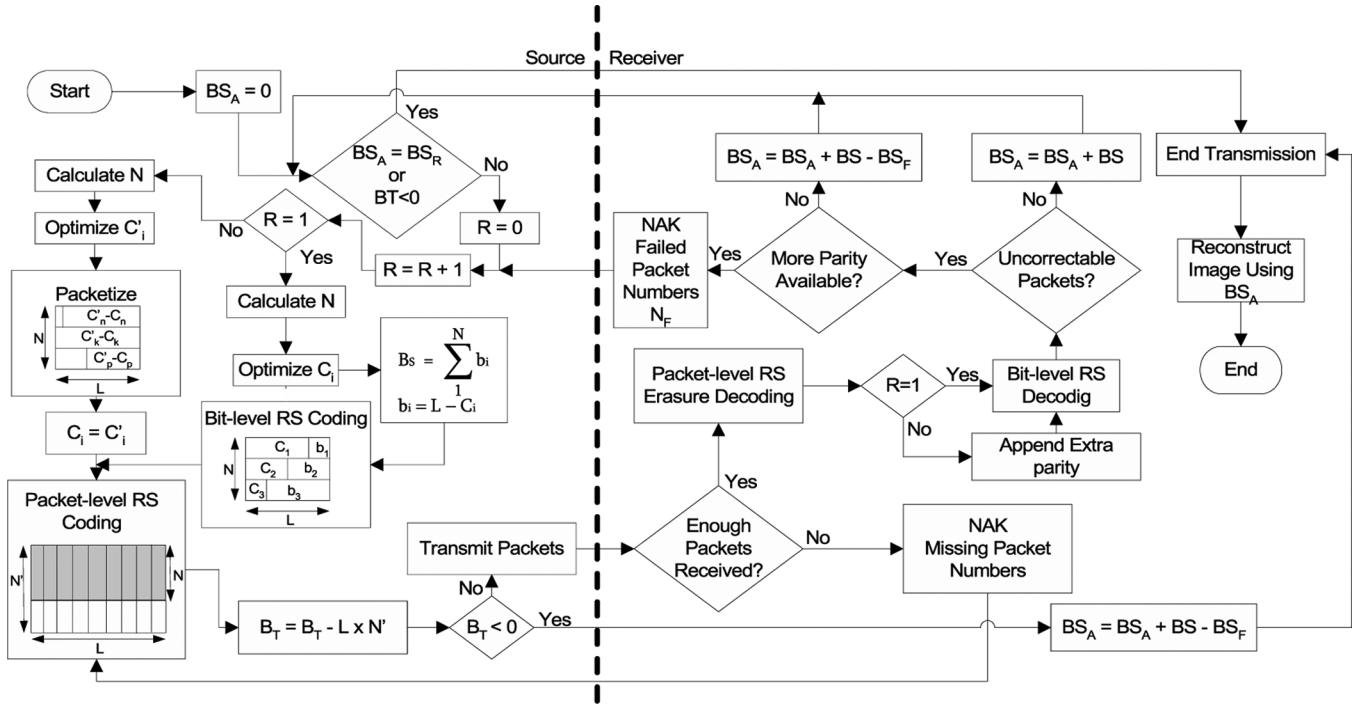
Fig. 1. Flowchart of the proposed end-to-end protocol.

packets, we note that each packet will contain source coding and channel coding or parity bits. The calculation of parity bits is done based on minimizing the expected distortion of the reconstructed bitstream. While the details of distortion minimization are discussed in Section IV, we note that the minimization can be carried out for both variable length and fixed-length packets. We consider the case of fixed-length packets in our implementation because it is more challenging and convincingly more practical from the standpoint of underlying network protocols such as ATM or even UDP/IP. Further, we propose the use of packet level channel coding to compensate for the packet erasure impacts on the packetized bitstream. Such coding scheme treats the collection of information and parity bits in each packet as data for the purpose of packet erasure compensation. However with the exception of an interleaving operation, there is no significant difference between compensating for bit errors and packet erasures from the standpoint of channel coding.

Our integrated protocol is categorized under type II hybrid Automatic Repeat reQuest (ARQ) and Forward Error Correction (FEC) protocols. In a type II hybrid protocol, a retransmission request is responded by transmitting a codeword containing extra parity bits for a previously transmitted codeword. Relying on the discussion of RS codes in [43] and [7] together with receiver feedback and erasure decoding, we propose the use of systematic rate compatible punctured RS codes in our protocol to compensate for both random bit errors and packet erasures. We note that the systematic rate compatible punctured RS codes together with erasure decoding outperform non-systematic RS codes of [21].

Fig. 1 depicts the flowchart of our end-to-end protocol. We assume that a bit budget B_T and a per round probability of delivering a packet set Π are given. Our round-based protocol, with variable R keeping track of the round number, consists

of two components. The first component or the outer loop is used to compensate for random bit errors. The second component or the inner loop is utilized to recover erased packets. In the first round, a bitstream is initialized to the progressively encoded image data.

Assuming a fixed packet length of L, a bitstream size of BS_R generated by the image coder, and a total of BS_A source coding bits delivered so far, the number of packets to transmit the bitstream is chosen as $N = \min(\lfloor \alpha B_T/L \rfloor, \lfloor BS_R - BS_A/L \rfloor, N_{Max})$ where $0 < \alpha < 1$ is a design parameter effectively splitting the available budget B_T between the two components of the protocol and N_{max} is a per round upper bound on the number of transmitted packets. The number of per packet parity symbols minimizing the expected distortion of the image under bit errors only is then calculated according to the discussion of Section IV. For packet i in the set of N formed packets, quantities b_i and C_i represent the number of bits allocated to source coding and parity, respectively. Next, the total number of data and parity packets N' required to statistically guaranteeing the delivery of the packet set is calculated according to the discussion of Section V. After updating transmission budget B_T, announcing the start time and the duration of the round, the source proceeds with the transmission of the coded packet set to the receiver. Each packet includes a sequence number. The receiver waits for the duration of the round before determining whether it has received N packets required to recover the packet set. The variable BS tracks the total number of source coding bits embedded in the packet set. At the end of the round, the receiver sends the packet numbers of the erased packets to the source in a single packet NAK message if it has not been able to recover the block of packets. We also note that utilization of similar error detection and correction codes along with the

employment of timeout mechanisms can effectively cope with the impacts of random bit errors and packet erasures in the transmission of single packet NAK and control messages. For simplicity, we assume that the transmission of single packet NAK and control messages are error free in the rest of our discussion. The NAK message includes a two bit per packet bitmap associated with the individual packets of the set. The receiver sets the MSB bit associated with a packet to zero if it has been able to recover the packet. With the MSB bit set to one, the receiver sets the LSB bit to one if it has not been able to recover the packet due to an erasure. The source then retransmits an extra number of packets in order to compensate for packet erasures in the channel. The number of extra packets is again calculated from the statistical guarantee algorithm of Section V. Notice that the RS code applied to the columns is also a rate compatible punctured RS code, and extra redundant packets can be generated if necessary. Because of the Maximum Distance Separable (MDS) property of RS codes [43], any N received packets can be used in the RS erasure decoder to recover the first N packets and the packet loop can be terminated. Once the receiver has recovered the block of packets, it aims at recovering the source coding bits in each packet. In the first round, each packet contains source coding bits and parity bits and is directly decoded to recover the data. In the second and later rounds, each packet includes incremental redundant bits. The variable C_i' indicates the total number of parity packets received in multiple rounds associated with the source coding bits of the original packet i. The receiver thus needs to append them to the previously uncorrectable packets. In either case, the contents of the receiver buffer are decoded. If there are no uncorrectable packets and BS_A is less than BS_R, another set of rounds is initiated starting from the first round. However, if N_F uncorrectable packets exist containing a total of BS_F source coding bits, the receiver requests extra redundant bits for those packets. If uncorrectable packets exist but their RS code has reached the length of the mother code, the transmission of the current set is started from the first round after checking the available budget. Otherwise, another round of delivering extra redundant bits initiates. The amount of redundancy is determined by increasing the error correcting capability of each packet of the first round to an amount calculated from the optimization algorithm of Section IV for the second round and beyond. Next, the source packetizes extra parity bits using appropriate header paddings and choosing $N = \min(N_F, \lfloor \alpha B_T/L \rfloor, N_{Max})$. It will then transmits the packets to the receiver. The entire set of rounds and consequently the image transmission terminate under one of the two following conditions: 1) the entire bitstream of the size BS_R has been received with no uncorrectable blocks, and 2) the transmission budget is exhausted. The image is reconstructed using all of the packets preceding the first uncorrectable packet immediately after the transmission is terminated.

In Sections III–V, we provide a detailed description of the components of our protocol.

III. CHANNEL CODING AND LOSS ANALYSIS

In this section, we first describe the properties of our proposed channel coder. We then continue by discussing the impacts of

utilizing multiple antennas. We finish this section by providing an analysis of temporally correlated channel loss relying on the Bernoulli and Gilbert–Elliott [12], [15] models.

In a round-based transmission scheme with R rounds, a rate compatible punctured RS channel coder converts k information symbols (packets) into a sequence of n_i-symbol (n_i-packet) blocks where $i = 1, \ldots, R$. Each symbol consists of a number of bits and each packet consists of a number of symbols. For the first sequence, $(n_1 - k)$ parity symbols (packets) are appended to k data symbols (packets). The sequences n_j for $j = 2, \ldots, R$ are obtained by appending $n_j - n_{j-1}$ symbols (packets) to the previous n_{j-1} symbols (packets). We also note that a combined channel code n_i is capable of correcting up to $\lfloor n_i - k/2 \rfloor$ errors when applied to symbols and up to $n_i - k$ errors when applied to packets.

In order to calculate the error rate of an $RS(n, k)$ coder block, we utilize a hybrid model consisting of the single-state Bernoulli and the two-state Gilbert–Elliott (GE) error models. In our discussion below, we describe the modulation symbol error rate and channel coding symbol loss rates. We distinguish between the two types of symbols by noting that a channel coding symbol typically consists of a number of modulation symbols. For example, an 8-bit RS channel coding symbol may consist of eight BPSK modulation symbols.

A. Calculation of the Symbol Error Rate for Multiple Antenna Systems

In [45], the authors calculate closed-form expressions describing the modulation symbol error rate φ of a multiple-transmit multiple-receive antenna system in terms of the number of signal points in the constellation M and the average signal-to-noise ratio SNR. We carry out our calculations under the assumption of facing a slow fading Rayleigh channel and utilizing the PSK modulation scheme. In what follows we provide a brief review of our discussion. First, we introduce the symbol error rate of a single-transmit N-receive antenna system using Maximum Ratio Combining (MRC) as

$$
\begin{aligned}
\varphi = \frac{M-1}{M} &- \frac{1}{\pi}\sqrt{\frac{\vartheta}{1+\vartheta}} \\
&\times \left\{ \left(\frac{\pi}{2} + \tan^{-1}\xi\right) \sum_{j=0}^{N-1} \binom{2j}{j} \frac{1}{[4(1+\vartheta)]^j} \right. \\
&+ \sin(\tan^{-1}\xi) \sum_{j=1}^{N-1}\sum_{i=1}^{j} \frac{\sigma_{ij}}{(1+\vartheta)^j} \\
&\left. \times [\cos(\tan^{-1}\xi)]^{2(j-i)+1} \right\}
\end{aligned} \tag{1}
$$

where $\vartheta = SNR \sin^2(\pi/M)$, $\xi = \sqrt{\vartheta/1+\vartheta}\cot\pi/M$, and $\sigma_{ij} = \binom{2j}{j} / \binom{2(j-i)}{j-i} 4^i [2(j-i)+1]$. From (1), one can calculate the symbol error rate of a single-transmit single-receive antenna system as well as a single-transmit double-receive antenna system by setting N to 1 and 2, respectively. Relying on a discussion of diversity gains, we also argue that the modulation symbol error rate of the Space–Time Block Codes (STBCs) of [2] and [40] can be calculated from (1) by proper mapping of the values of SNR. For example, the symbol error rate of

a double-transmit single-receive antenna system can be calculated by replacing SNR with $SNR/2$ and setting N to 2 in (1). Similarly, the symbol error rate of a double-transmit double-receive antenna system can be calculated by replacing SNR with $SNR/2$ and setting N to 4 in (1).

B. Discussion of the Hybrid Loss Model

As pointed out in many research articles, the pattern of random bit errors in a fading wireless channel is bursty representing temporal correlation. The two-state GE loss model provides an elegant mathematical model to capture the error pattern of such channel. In the GE model, the loss of a bit is described by a two-state Markov chain. The two states are denoted by state G and B. State G represents a bit error rate of ε_G while state B represents a bit error rate of ε_B where $\varepsilon_B \gg \varepsilon_G$. State G also introduces a self-transitioning probability of γ and a transitioning probability of $1 - \gamma$ to state B. Similarly, state B introduces a self-transitioning probability of β and a transitioning probability $1 - \beta$ to state G. Per state bit error rates of the GE model ε_G and ε_B can be expressed as a function of modulation symbol error rates φ_G and φ_B. For example, for the BPSK modulation scheme, i.e., $M = 2$ in (1), $\varepsilon_G = \varphi_G$ and $\varepsilon_B = \varphi_B$. The parameters γ and β can be typically measured from the observed loss rates and average burst lengths of the channel [18].

For the GE loss model, the probability of receiving exactly k bits from n transmitted bits is described by

$$P(n, k) = P(n, k, G) + P(n, k, B). \qquad (2)$$

Further, the recursive probabilities of receiving exactly k bits from n transmitted bits and winding up in state G and B are respectively given by

$$
\begin{aligned}
&P(n, k, G) \\
&= \varepsilon_G[\gamma P(n-1, k, G) + (1-\beta)P(n-1, k, B)] \\
&\quad + (1 - \varepsilon_G) \\
&\quad \times [\gamma P(n-1, k-1, G) + (1-\beta)P(n-1, k-1, B)]
\end{aligned}
$$
$$(3)$$

and

$$
\begin{aligned}
&P(n, k, B) \\
&= \varepsilon_B[(1-\gamma) P(n-1, k, G) + \beta P(n-1, k, B)] \\
&\quad + (1 - \varepsilon_B) \\
&\quad \times [(1-\gamma)P(n-1, k-1, G) + \beta P(n-1, k-1, B)]
\end{aligned}
$$
$$(4)$$

for $n \geq k > 0$ and the initial conditions

$$
\begin{aligned}
P(0, 0, G) &= & g_{ss} &= \frac{1-\beta}{2-\gamma-\beta} \\
P(0, 0, B) &= & b_{ss} &= \frac{1-\gamma}{2-\gamma-\beta} \\
P(1, 0, G) &= & \varepsilon_G[\gamma g_{ss} + (1-\beta)b_{ss}] \\
P(1, 0, B) &= & \varepsilon_B[(1-\gamma)g_{ss} + \beta b_{ss}]
\end{aligned}
$$
$$(5)$$

In what follows, we model the loss pattern of the channel coding symbols under the assumption that the loss pattern of the communication channel at the bit level is described by the GE model. Suppose the RS coder generates a set of channel coding
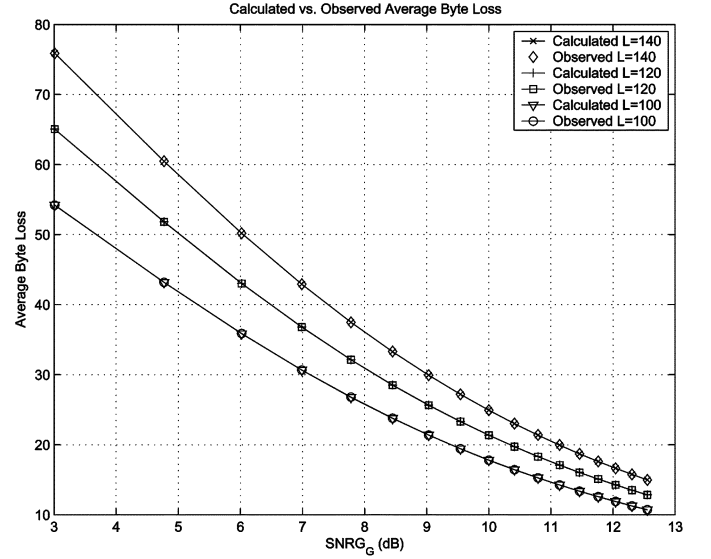

Fig. 2. Comparison of calculated and observed average byte loss for a channel coding symbol size of eight bits and BPSK modulation.

symbols where each symbol consists of s bits. A channel coding symbol is received error free if all of its s bits are received free of errors. The probability of receiving a channel coding symbol free of error under the GE model is obtained from (2) with $n = k = s$ as $P(s, s)$. Note that we assume not having access to the information about the initial bit of a given channel coding symbol and hence also capturing the inter-symbol temporal correlation in the expression $P(s, s)$. Relying on a hybrid loss model in which inter-symbol temporal correlation is not deemed significant compared to intra-symbol temporal correlation, we can obtain the probability of channel coding symbol block loss from

$$\Psi(n, t_C, \varepsilon) = \sum_{i=0}^{n-t_C-1} P(n, i) = \sum_{i=0}^{n-t_C-1} \binom{n}{i} \varepsilon^{(n-i)}(1-\varepsilon)^i$$
$$(6)$$

where $\varepsilon = 1 - P(s, s)$. It is important to note that in (6), the probabilities of receiving error free channel coding symbols $P(s, s)$ are calculated independently for each channel coding symbol but intra-symbol temporal correlation is captured in the calculation of $P(s, s)$.

Next, we experimentally validate our hybrid loss model. Fig. 2 provides sample validation results of our hybrid loss model. For a channel coding symbol size of eight bits, BPSK modulation, and three different choices of transmitted byte lengths L, the figure compares the calculated average byte loss from our hybrid model with the observed average byte loss over a range of values of SNR_G in the GE model with $SNR_G = 10SNR_B$. The other parameters of the GE model are set as $\gamma = 0.99873$ and $\beta = 0.875$ representing a burst length of eight. The averages are calculated over one million experiments. As observed from the plots, the values of calculated and observed average byte loss match in all three cases. Note that while the choice of channel coding symbol size affects our validation results, the error correcting capabilities of the utilized channel coding scheme has no effect on our results. While not shown here, we have observed consistent results in

a large set of validation experiments for a variety of the GE model parameter settings.

At the end of this section, we note that the Gilbert model of [15] with trivial per state error probabilities of $\varepsilon_G = 0$ and $\varepsilon_B = 1$ is used to describe the packet loss of the underlying channel.

IV. BIT ERROR CORRECTION

In this section, we discuss the protection of the source coding bits in a packet set associated with a progressive bitstream. The bitstream is packetized into a number of packets with fixed-lengths. In order to protect source coding bits against random bit errors, we propose the use of rate compatible punctured RS error correction codes in each packet. As pointed out in Section II, our protocol calls for an ordered round-based transmission of packet sets. Leaving the details of compensating for packet erasures to the next section, we discuss the details of random bit error compensation going from one round to another in this section. Hence, the main goal of this section is to introduce an optimization framework that minimizes the expected distortion of the reconstructed image due to random bit errors in a single round of transmission.

A. Optimization Formulation

Consistent with Section II, we assume the original size of the bitstream generated by the image source is BS_R and so far BS_A bits of the bitstream have been delivered. Hence, the remaining number of the bits in the bitstream have to be packetized into N fixed-length packets with length L. The choice of packet length L has to avoid segmentation in the data link, network, and transport layer protocols in order to preserve the effectiveness of channel coding operation at the bit level.

Once the packet length L is chosen, the number of packets N for the first round is selected such that the collection of packets contains a number of source coding bits less than or equal $BS_R - BS_A$. We set $N = \min(\lfloor \alpha B_T / L \rfloor, \lfloor BS_R - BS_A / L \rfloor, N_{Max})$ where the parameters are defined in Section II. Denoting b_i and C_i respectively as the source and the channel coding bits associated with packet i for $i \in \{1, \ldots, N\}$, we observe that $b_i + C_i = L$. We recall that utilizing our proposed channel coding scheme introduces a channel code rate of $r_i = b_i / L$ for packet i. The optimization problem is aimed at finding the parity assignment of each packet C_i such that a measurement of the expected distortion is minimized. The expected distortion can be calculated as the probabilistic average of distortions associated with recovering the first $i - 1$ packets in a given packet set and failing to recover packet i with $i \in \{1, \ldots, N + 1\}$. Generally speaking, the distortion of events associated with recovering consecutive packets are not mutually independent for a channel with memory. However, the use of the hybrid loss model of the previous section allows us to assume such events are mutually independent with a relative accuracy. Thus, the expected distortion can be expressed as

$$\mathcal{E}[D] = D_0 \Psi_1 + \sum_{i=2}^{N+1} \Psi_i D_{i-1} \prod_{j=1}^{i-1} (1 - \Psi_j). \qquad (7)$$

In (7), Ψ_i with $i \in \{1, \ldots, N\}$ is the failure probability of recovering packet i, $\Psi_{N+1} \triangleq 1$, D_i with $i \geq 1$ is the distortion of a reconstructed image with the first i packets, and $D_0 = \sigma^2$ is the source variance. The distortion D_i is a function of the aggregate received bits $\Upsilon_i = \sum_{j=1}^{i} b_j$. While the data associated with the function D_i can be extracted directly from SPIHT or other coders, it can also be approximated utilizing data fitting techniques. The advantage of using a closed-form approximated function for distortion is to reduce the time complexity of our optimization problem. In [3], the authors propose an approximation of the rate-distortion function of the SPIHT codec in the form of

$$D_i(\Upsilon_i) = \sum_{j=1}^{4} h_j e^{-l_j \Upsilon_i} \qquad (8)$$

where h_j and l_j are parameters that are identified independently for different classes of images. We note that the same approach can be used to approximate the rate-distortion function of other image codecs. Further, the probabilities Ψ_i for $i = \{1, \ldots, N\}$ can be expanded in terms of channel loss characteristics as described in Section II. In the case of utilizing the hybrid Bernoulli-GE loss model and calculating the bit error probability $\varepsilon = P(s, s)$, Ψ_i is calculated from (6) by setting $n = L$ and $t_C = \lfloor C_i / 2 \rfloor$. Making note that for the fixed-length packet i specifying the bits allocated to data b_i is equivalent to specifying the bits allocated to parity C_i, the optimization problem of the first round is expressed as

$$\min_{C_1, \ldots, C_N} \qquad \mathcal{E}[D] \qquad (9)$$

$$\text{Subject To}: \qquad \sum_{i=1}^{N} (L - C_i) \leq BS_R - BS_A \qquad (10)$$

$$0 \leq C_i < L, \quad i \in \{1, \ldots, N\}. \qquad (11)$$

While Constraint (10) shows that the number of source coding bits in the N packets adds up to no more than the number of bits in the remaining part of bitstream, Constraint (11) places a lower and an upper bound on the per packet channel coding bits. We note that the problem of (9) is subject to discrete constraints applied to available channel coding variables $C_1, \ldots, C_N$. It is hence categorized under Mixed Integer NonLinear Programming (MINLP). Under the assumption of feasibility, the solution to the standard problem can provide a close estimate of the MINLP solution. Assuming the solution to the optimization problem of the first round specifies a per packet set of channel coding bits $\{C_1, \ldots, C_N\}$ and source coding bits $\{L - C_1, \ldots, L - C_N\}$, the optimization problem of the rounds beyond the first round are specified with the same cost function as (7) for the per packet source coding bits of the first round but a different number of channel coding bits, $\Psi_i = 0$ for previously delivered packets, and the following constraint set:

$$\sum_{i \in \mathcal{F}} (C_i' - C_i) \leq NL \qquad (12)$$

$$C_i' = C_i, \quad i \in \mathcal{R} \qquad (13)$$

$$C_i \leq C_i' \leq L_{max} - (L - C_i), \quad i \in \mathcal{F} \qquad (14)$$

where $N = \min(N_F, \lfloor \alpha B_T/L \rfloor, N_{Max})$, L_{max} is the mother code length, $\mathcal{F}$ and $\mathcal{R}$ indicate the set of failed and recovered packets, C_i and C_i' with $i \in \mathcal{F} \cup \mathcal{R}$ denote the current and the previous collective number of parity bits for packet i, respectively. While the formulations of this section specify a distortion-optimal problem, they can be easily changed to reflect a rate-optimal problem. Further, we note that the formulation of (9) can be applied to a variable-length packet scenario in which the number of data bits in a packet is fixed and the number of parity bits are obtained by solving the optimization problem. In the rest of our discussion, we focus on the distortion-optimal problem of (9) along with the constraint set (10) and (11) for a fixed-length packet scenario.

B. Optimization Solution

In this section, we provide a discussion of solving the optimization problems of Section IV-A. Relying on the Lagrangian theory [6], we convert the problem of the first round to an optimization problem without constraints. We define the Lagrangian function of (9) as

$$LG_D = \mathcal{E}[D] + \lambda \left(NL - \sum_{i=1}^{N} C_i - BS_R + BS_A \right) + \mu_1(C_1 - L) + \cdots + \mu_N(C_N - L) \quad (15)$$

where the parameters λ, $\mu_1, \ldots,$ and μ_N are the Lagrange multipliers in the Lagrangian (15). The unconstrained minimization problem for $\Omega = \{C_1, \ldots, C_N\}$ is defined as

$$\min_{\Omega} LG_D = \min_{\Omega} \left\{ \mathcal{E}[D] + \lambda \left(NL - \sum_{i=1}^{N} C_i - BS_R + BS_A \right) + \sum_{i=1}^{N} \mu_i(C_i - L) \right\} \quad (16)$$

where $\Omega = \{C_1, \ldots, C_N\}$ and the parameters $\lambda, \mu_1, \ldots, \mu_N$ are the Lagrange multipliers.

Taking into consideration the discrete nature of our problem and considering the fact that (9)–(11) are convex[1], we propose deploying Sequential Quadratic Programming (SQP) technique to solve the problem. In SQP, the necessary conditions for optimality are represented by Karush–Kuhn–Tucker (KKT) conditions described below.

$$\nabla LG_D(\Omega^*)$$
$$= \left[\frac{\partial LG_D}{\partial C_1^*}, \ldots, \frac{\partial LG_D}{\partial C_N^*}, \frac{\partial LG_D}{\partial \lambda^*}, \frac{\partial LG_D}{\partial \mu_1^*}, \ldots, \frac{\partial LG_D}{\partial \mu_N^*} \right] = 0$$
$$\lambda^* \left(NL - \sum_{i=1}^{N} C_i^* - BS_R + BS_A \right) = 0$$
$$\mu_i^*(C_i^* - L) = 0$$
$$\lambda^*, \mu_i^* \geq 0. \quad (17)$$

[1]The function $f : \mathcal{C} \longmapsto \mathcal{R}^n$ defined over the convex set $\mathcal{C} \subseteq \mathcal{R}^n$ is called convex if $\forall x_1, x_2 \in \mathcal{C}$ and $0 \leq \eta \leq 1$ the inequality $f(\eta x_1 + (1 - \eta)x_2) \leq \eta f(x_1) + (1 - \eta)f(x_2)$ holds.

Further, $\lambda^*, \mu_i^* \geq 0$ for $i = 1, \ldots, N$ if associated with an active inequality at the optimal point Ω^*, i.e.,

$$\begin{cases} \lambda^* \geq 0 : & \text{if } \sum_{i=1}^{N} C_i^* = NL - BS_R + BS_A \\ \lambda^* = 0 : & \text{otherwise} \end{cases} \quad (18)$$

$$\begin{cases} \mu_i^* \geq 0 : & \text{if } C_i^* = L \\ \mu_i^* = 0 : & \text{otherwise.} \end{cases} \quad (19)$$

A variant of the quasi-Newton method [31] can then be used to iteratively find the solution to the optimization problem. We note that utilizing a variant of the quasi-Newton method is equivalent to solving a quadratic estimation of the problem in every iteration. The time complexity of solving the optimization problem is $\mathcal{O}(Id \log d)$ where I indicates the number of iterations and d indicates the degree of the overall quadratic estimation[2]. The solution to the optimization problem of the second round and beyond is similar and is skipped here. We have observed that an average of ten and no more than twelve iterations are required for the convergence of our proposed optimization algorithm of the first round. The associated numbers for the algorithm of the second round and beyond depend on the number of lost packets but are generally smaller than the ones in the first round. Hence, the worst case complexity results are quite good compared to other recursive optimization approaches such as dynamic programming introducing a worst case time complexity in the order of $\mathcal{O}(d^2)$.

At the end of this section, it is important to note that our optimization approach is loosely coupled with the choice of error model through the choice of coefficients Ψ_i in (7). While in our work the expressions of Ψ_i are calculated relying on the expressions of (6), (2), (3), and (4) for the hybrid Bernoulli–GE loss model, one can work with an alternate error model such as a finite-state Markov chain model by updating the expressions of Ψ_i accordingly. Thus, our optimization approach can be transparently used in conjunction with any error model.

V. STATISTICAL RECOVERY FROM PACKET ERASURES

We now turn our focus on the statistical recovery of the packets associated with the bitstream of a progressive source coder in an erasure channel. We assume that the individual packets of the set contain both source coding and parity bits. For the purpose of packet erasure compensation, we treat the collection of source coding and parity bits as data. Focusing on ordered delivery of consecutive packet sets, we propose utilizing rate compatible punctured RS codes at the packet level to compensate for packet erasures. However, our approach in this section relies on providing a statistical guarantee for delivering a packet set. The term statistical guarantee of the packet set delivery is used to indicate that a packet set can be successfully delivered with a probability better than a given threshold assuming the specifications of the packet erasure channel are known. Our earlier work of [44] introduces the following algebraic placement algorithm with a time complexity of $\mathcal{O}(zk)$ to calculate the smallest number of required transmitted packets $u = k + z$ in order to guarantee the receipt

[2]We note that the optimization problem can also be solved relying on a table look up approach in case distortion data is directly read from SPIHT coder as oppose to relying on the approximated function of (8).

of at least k packets with a probability Π or better for a system governed by the Gilbert loss model.

Statistical Guarantee for Packet Delivery Algorithm

• Initialize $\Phi(k,k) = \gamma^k \frac{1-\beta}{2-\gamma-\beta} + \gamma^{k-1}(1-\beta)\frac{1-\gamma}{2-\gamma-\beta}$

• for $(z = 1 \text{ to } k)\{$

   — Calculate $P(k+z,k)$

   — Update $\Phi(k+z,k) = \Phi(k+z-1,k) + P(k+z,k)$

   — If $\Phi(k+z,k) \geq \Pi$, then Break

  $\}/*$ for $(z = 1 \text{ to } k)*/$

• Report the number of required packets, $n = k + z$

The quantities of interest in the algorithm above are described as follows. $P(k+z,k)$ the probability of receiving k packets from $k+z$ transmitted packets is given by (2) and recursive (3) and (4) in the case of utilizing Gilbert model. Further, $\Phi(k+z,k)$ the probability of receiving k packets or more from $k+z$ transmitted packets is defined as

$$\Phi(k+z,k) = \sum_{i=k}^{k+z} P(k+i,i). \qquad (20)$$

It is important to note that there is a one-to-one relationship between the choice of the parameter Π in our statistical guarantee algorithm and the bandwidth split factor parameter α. In other words, specifying one of the parameters automatically identifies the other parameter.

It also is important to note that the choice of error model does not affect the operation of the algorithm described above. By calculating the values of $P(k+z,k)$ from the recursive or closed-form expressions of an alternate error model of choice, one can utilize that error model instead of the Gilbert model.

VI. NUMERICAL ANALYSIS

In this section, we present our simulation results based on the protocol of Section II and the discussion of the sections following it. For our simulation, we consider the transmission of SPIHT [30] encoded class of gray scale images including $512 \times 512 \times 8bpp$ Lena, Zelda, and Barbara images over a channel characterized by correlated loss.

In our experiments, we use rate compatible punctured RS codes with a maximum length 255 over $GF(256)$ and a symbol size of 8 bits. We utilize hybrid Bernoulli-GE and Gilbert loss models to describe bit errors and packet erasures, respectively. We set the transition probabilities of both models as $\gamma = 0.99873$ and $\beta = 0.875$ corresponding to an average burst length of 8. Besides the trivial choice of error probabilities in the case of Gilbert model, per state error probabilities of the GE model are calculated based on the results of (1) for BPSK modulation with $M = 2$ and $SNR_G = 10SNR_B$. Hence, we set $\varepsilon_G = \varphi_G$ and $\varepsilon_B = \varphi_B$ in our hybrid Bernoulli-GE error model. Further, we set $N_{Max} = 50$ and $BS_R = 512 \times 512/8$ Bytes for a compression ratio of 8. For our statistical packet delivery algorithm, we set
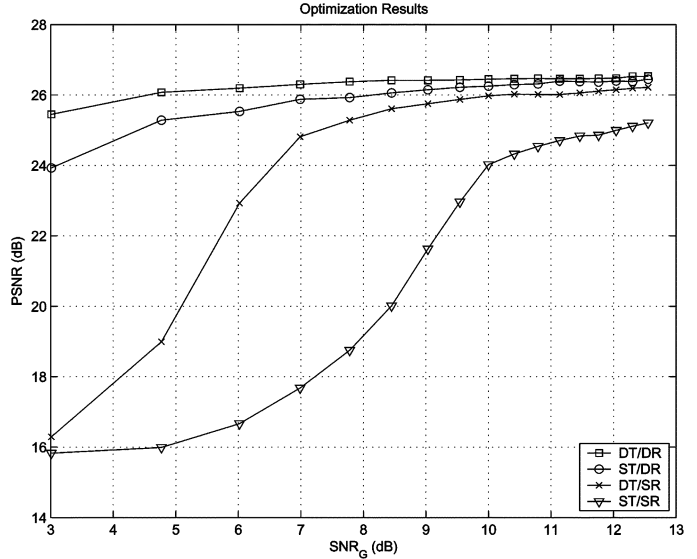

Fig. 3. Open-loop plots of $PSNR$ versus SNR_G in the case of Lena image for four different antenna configurations.

$\Pi = 0.9988$ translating to $\alpha = 0.72$. Our choices of packet lengths guarantee that there is no segmentation/reassembly of UDP or ATM packets over Ethernet and/or IEEE 802.11 frames. This is due to the fact that transmitting UDP/IP packets on top of Ethernet and IEEE 802.11 frames introduces a maximum allowable packet size of $L = 1476$ Bytes without facing segmentation. The set of parameters associated with the Lena image in (8) are set as $(h_1,h_2,h_3,h_4,l_1,l_2,l_3,l_4)=$ $(1276.7, 117.2, 26.9, 279.1, 331.85, 11.27, 1.58, 50.28)$. Similarly, the set of parameters for Zelda and Barbara images are set as $(1144.5,175.91,13.57,52.68,393.52,61.55,1.24,12.93)$ and $(1337.1,391.71,272.96,97.43,531.91,76.00,8.33,2.22)$, respectively.

We validate and present our results as follows. First, we study the behavior of our single round protocol without receiver feedback. We refer to the latter scenario as an open-loop scenario. We conduct our open-loop experiments for an erasure free channel and a channel with packet erasures. Second, we look at the behavior of our multiple round protocol with receiver feedback to which we refer to as a closed-loop scenario.

A. Open-loop Results

In an open-loop scenario, we transmit a bitstream in a single round and evaluate the quality of the reconstructed image at the receiver. We start by transmitting the bitstream over an erasure free channel. We have two compelling reasons to study the behavior of our protocol for such a scenario. First, we are able to validate the effectiveness of our bit error optimization scheme. Second, we can show the mere advantage of utilizing multiple antenna transmission. While this section only reports our results in the case of Lena image, we have obtained similar results in the case of other images including Zelda and Barbara.

Fig. 3 compares the plots of $PSNR = 10\log_{10} 255^2/\mathcal{E}[D]$ versus SNR_G in the case of Lena image for a packet length of $L = 100$ Bytes, $B_T = 5,000$ Bytes, and four antenna configurations: 1) a Single-Transmit Single-Receive (ST/SR) antenna system, 2) a Double-Transmit Single-Receive (DT/SR) antenna
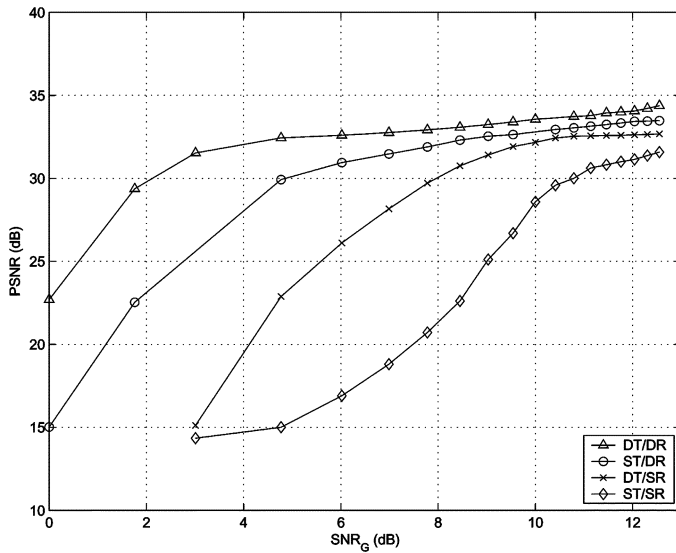
Fig. 4. Closed-loop plots of $PSNR$ versus SNR_G in the case of Lena image for four different antenna configurations.

Fig. 5. Closed-loop plots of $PSNR$ versus SNR_G in the cases of (a) Zelda and (b) Barbara images for four different antenna configurations.

system, 3) a Single-Transmit Double-Receive (ST/DR) antenna system, and 4) a Double-Transmit Double-Receive (DT/DR) antenna system. For a fair comparison, all systems use the same transmission power. Every point in the curves indicates an average value taken over 20 simulations. While not shown here, the expected values of $PSNR = 10 \log_{10} 255^2 / \mathcal{E}[D]$ match the real values of $PSNR = 10 \log_{10} 255^2 / D$ observed in our experiments with an accuracy of no worse than 2 dB.

Comparing the results of the figures, we observe that the $PSNR$ of a DT/DR antenna system is higher than that of the rest. In addition, the $PSNR$ of an ST/SR antenna system is lower than that of the rest. Comparing the $PSNR$ of an ST/DR antenna system with that of a DT/SR antenna system, we observe that the former introduces a higher $PSNR$. From the results of [45], we recall that the diversity gain is in the order of the product of the transmit and the receive antennas. Hence, both ST/DR and DT/SR scenarios achieve a diversity gain of order two. However, from the signal-to-noise ratio standpoint the efficiency of the latter scenario suffers a 3 dB loss compared to that of the former scenario because the transmission power is divided between antennas. This justifies the higher $PSNR$ of an ST/DR antenna system compared to that of a DT/SR antenna system. Since the channel coding effects saturate beyond a certain SNR_G, we also observe that the performance advantage of utilizing multiple antennas in lower values of SNR is more significant than that of higher values of SNR. However due to lack of packet erasures, the expected quality is relatively good in all four cases even with the small transmission budget of 5000 Bytes.

B. Closed-Loop Results

In this section, we study the performance of our closed-loop protocol over a channel introducing bit errors and packet erasures. With the exception of $B_T = 20,000$ Bytes, we apply identical settings of other parameters as before to our experiments.
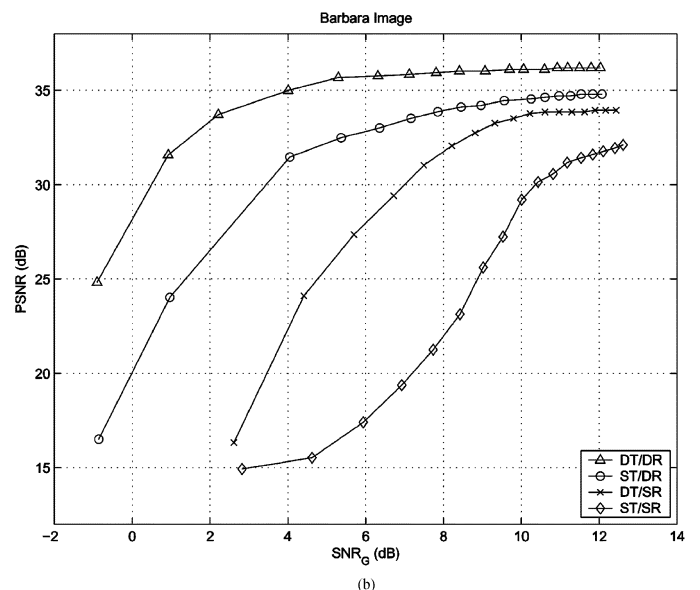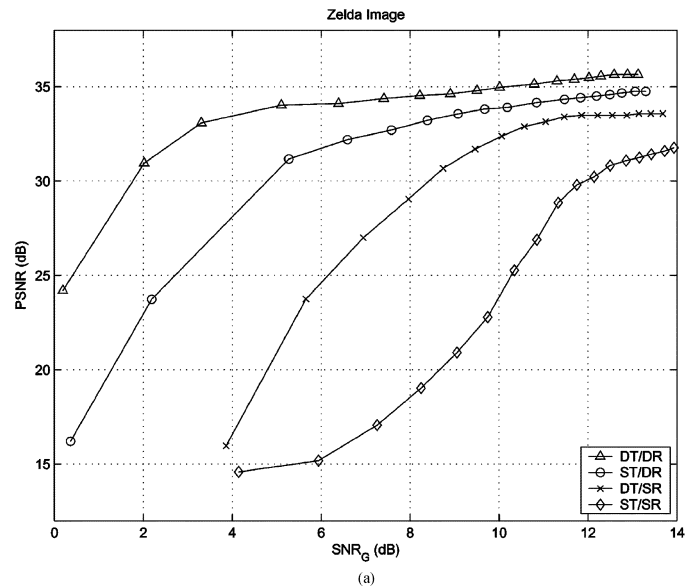
We start by investigating the effects of utilizing different combinations of multiple antennas in the transmitter/receiver pairs. Figs. 4 and 5 show the plots of $PSNR = 10 \log_{10} 255^2 / D$ versus SNR_G in the case of Lena, Zelda, and Barbara images for the four antenna configuration scenarios, ST/SR, DT/SR, ST/DR, and DT/DR. Comparing the results of figures, we observe the same qualitative pattern of behaviors as our open-loop experiments. The best quality is achieved by DT/DR configuration followed by ST/DR, DT/SR, and ST/SR. In all of the curves, there is almost a linear transition regime from a low quality region to a high quality region. The quality of the reconstructed image remains in a low quality region for any choice of SNR_G below a low threshold. As SNR_G increases, the quality improves until reaching to a high threshold. The quality of the reconstructed image remains in a high quality region for any choice of SNR_G beyond the high threshold.
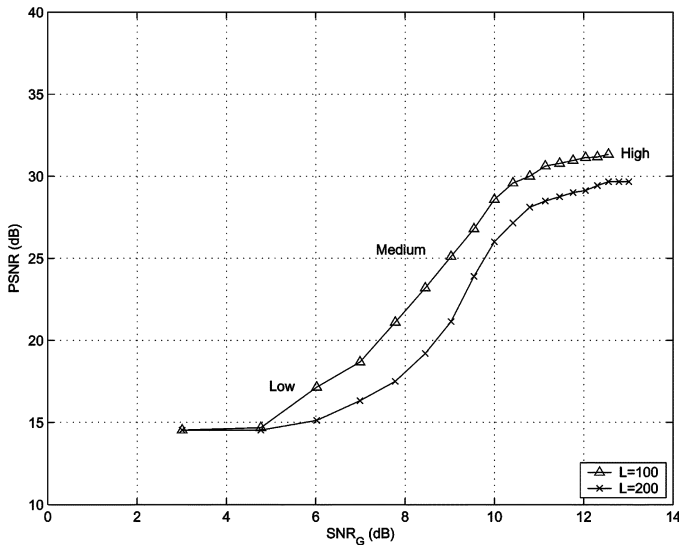
Fig. 6. ST/SR closed-loop plots of $PSNR$ versus SNR_G in the case of Lena image for two different choices of the packet size.

Fig. 7. Comparison of the original and reconstructed sample Lena images of the ST/SR plots of Fig. 6 utilizing $L = 100$ Bytes. Clockwise from the top left: the original image, the reconstructed image at SNR_G equal to 6 dB, 9 dB, and 13 dB, respectively.

Albeit the existence of packet erasures, the main difference compared to our open-loop results is that because of the higher transmission budget of 20 000 Bytes in closed-loop cases and the use of feedback the quality of reconstructed images have improved by a factor of up to 4 dB in $PSNR$ scale compared to their open-loop case. Once again, our experiments indicate the performance advantage of utilizing multiple antennas in the same order observed in our open-loop experiments with the amount of performance gain depending on the value of SNR_G. While for small values of SNR_G the neighboring curves are more than few dB's apart from each other in $PSNR$ scale, the difference for large values of SNR_G is less than 1 dB.

Next, we study the effects of the choice of packet size in the performance of our end-to-end protocol. Fig. 6 shows the plots of $PSNR = 10 \log_{10} 255^2/D$ versus SNR_G for two different values of the packet length L in the case of Lena image. For a given packet size, the plots describe how the quality of the reconstructed image improves as the average signal-to-noise ratio increases. Again, every point in the curves indicates an average value taken over 20 simulations. The plots show a similar pattern with different choices of the packet size. Once more, we observe a linear transition regime from a low quality region to a high quality region with the effect of larger packet sizes shifting the curve to the right. We also observe a slightly lower high quality value for $L = 200$ Bytes that can be potentially justified as the result of getting close to the maximum mother code length. Fig. 7 shows sample images corresponding to the low, medium, and high $PSNR$ regions in Fig. 6 for the choice of $L = 100$ Bytes.

In order to study the behavior of the protocol under different assignments of the bandwidth to the random bit error and packet erasure components of the protocol, we have also performed a set of open-loop experiments with different values of α in the range of $[0.2, 0.8]$ while keeping the other parameters fixed utilizing the class of images that includes Lena, Zelda, and Barbara images. While we do not report our results here due to lack of space, our experiments show similar qualitative behaviors as the ones reported here. The main observation is that for

a specific choice of α which is experimentally approximated to be 0.72, the performance results are optimized in terms of achieved $PSNR$. The results are more complicated in the case of closed-loop experiments although the same choice of α still represents an appropriate selection of the parameter. Exploiting the optimal choice of α is the subject of our future research work.

VII. CONCLUSION

In this paper, we presented a statistical optimization framework for multiple antenna transmission of progressive images over noisy channels. Relying on rate compatible punctured RS codes, our framework was able to compensate for random bit errors as well as packet erasures. We considered the impacts of transmission over channels with memory represented by a hybrid Bernoulli and Gilbert–Elliott model. In order to cope with random bit errors, we introduced an optimization framework to minimize the expected distortion of a reconstructed image. We were able to solve our optimization problem with a worst case time complexity better than that of dynamic programming and exhaustive search. Next, we provided an algorithm that was capable of statistically compensating for packet erasures. Relying on the receiver feedback, we integrated our bit error and packet erasure results in the form of a type II hybrid FEC-ARQ algorithm. Finally, we numerically validated our results by transmitting images over lossy channels characterized by temporally correlated loss. In addition we investigated the effects of multiple antenna diversity in transmission scenarios of progressive images over such channels. Simulation results demonstrated a great performance improvement as the result of using multiple antennas. Our future research work relates to the accommodation of real-time deadlines in our protocol framework for the transmission of video and point-to-multipoint transmission scenarios.

REFERENCES

[1] O. Açikel and W. Ryan, "Punctured turbo-codes for BPSK/QPSK channels," *IEEE Trans. Commun.*, vol. 47, no. 9, pp. 1315–1323, Sep. 1999.

[2] S. M. Alamouti, "A simple transmit diversity technique for wireless communications," *IEEE J. Sel. Areas Commun.*, vol. 16, no. 8, pp. 1451–1458, Oct. 1998.

[3] A. Appadwedula, D. L. Jones, K. Ramchandran, and I. Konzintsev, "Joint source channel matching for a wireless communications link," in *Proc. IEEE ICC*, 1998.

[4] A. H. Banihashemi and A. Hatam, "A distortion optimal rate allocation algorithm for transmission of embedded bitstreams over noisy channels," in *Proc. IEEE DCC*, 2007.

[5] B. A. Banister, B. Belzer, and T. R. Fischer, "Robust image transmission using JPEG2000 and turbo-codes," *IEEE Signal Process. Lett.*, vol. 9, no. 4, pp. 117–119, Apr. 2002.

[6] D. P. Bertsekas, *Nonlinear Programming*, 2nd ed. Belmont, CA: Athena Scientific, 1999.

[7] R. E. Blahut, *Algebraic Codes for Data Transmission*. Cambridge, U.K.: Cambridge Univ. Press, 2003.

[8] V. Chande, H. Jafarkhani, and N. Farvardin, "Joint-source channel coding of images for channels with feedback," in *Proc. IEEE Workshop on Information Theory*, 1998.

[9] V. Chande, H. Jafarkhani, and N. Farvardin, "Image communication over noisy channels with feedback," in *Proc. IEEE ICIP*, 1999.

[10] V. Chande and N. Farvardin, "Progressive transmission of images over memoryless channels," *IEEE J. Sel. Areas Commun.*, vol. 18, no. 6, pp. 850–860, Jun. 2000.

[11] P. C. Cosman, J. K. Rogers, P. G. Sherwood, and K. Zeger, "Combined forward error control and packetized zerotree wavelet encoding for transmission of images over varying channels," *IEEE Trans. Image Process.*, vol. 9, no. 6, pp. 982–993, Jun. 2000.

[12] E. O. Elliott, "Estimates on error rates for codes on burst-noise channels," *Bell Syst. Tech. J.*, Sep. 1963.

[13] F. Etemadi and H. Jafarkhani, "An efficient progressive bitstream transmission system for hybrid channels with memory," *IEEE Trans. Multimedia*, vol. 8, no. 6, pp. 1291–1298, Dec. 2006.

[14] N. Farvardin and V. A. Vaishampayan, "Optimal quantizer design for noisy channels: An approach to combined source-channel coding," *IEEE Trans. Inform. Theory*, vol. IT–33, no. 7, pp. 827–838, Nov. 1987.

[15] E. N. Gilbert, "Capacity of a burst-noise channel," *Bell Syst. Tech J.*, vol. 39, pp. 1253–1265, Sep. 1960.

[16] J. Hagenauer, "Rate compatible punctured convolutional (RCPC) codes and their applications," *IEEE Trans. Commun.*, vol. 36, no. 4, pp. 389–400, Apr. 1988.

[17] R. Hamzaoui, V. Stankovic, and Z. Xiong, "Optimized error protection of scalable image bit streams," *IEEE Signal Process. Mag.*, vol. 22, no. 6, pp. 91–107, Nov. 2005.

[18] H. Jafarkhani, P. Ligdas, and N. Farvardin, "Adaptive rate allocation in a joint source-channel coding framework for wireless channels," in *Proc. IEEE VTC*, Apr. 1996.

[19] J. Lu, A. Nosratinia, and B. Aazhang, "Progressive source-channel coding of images over bursty error channels," in *Proc. IEEE ICIP*, 1998.

[20] H. S. Malvar, "Fast progressive wavelet coding," in *Proc. IEEE DCC*, 1999.

[21] D. M. Mandelbaum, "An adaptive-feedback coding scheme using incremental redundancy," *IEEE Trans. Inform. Theory*, vol. IT-20, no. 3, pp. 388–389, May 1974.

[22] D. Rowitch and L. Milstein, "On the performance of hybrid FEC/ARQ systems using rate compatible punctured turbo (RCPT) codes," *IEEE Trans. Commun.*, vol. 48, no. 6, pp. 948–959, Jun. 2000.

[23] A. E. Mohr, E. A. Riskin, and R. E. Ladner, "Recovering from bit errors in scalar-quantized discrete wavelet transformed images," in *Proc. IEEE ICIP*, 1998.

[24] A. E. Mohr, E. A. Riskin, and R. E. Ladner, "Unequal loss protection: Graceful degradation over packet erasure channels through forward error correction," *IEEE J. Sel. Areas Commun.*, vol. 18, no. 6, pp. 819–828, Jun. 2000.

[25] E. Ordentlich, M. J. Weinberger, and G. Seeroussi, "A low complexity modeling approach for embedded coding of wavelet coefficients," in *Proc. IEEE DCC*, 1998.

[26] J. L. Perez-Cordoba, V. G. Ruiz, and I. Garcia, "Progressive image transmission over a noisy channel using wavelet transform and channel optimized vector quantization," in *Proc. IEEE ICIP*, 2002.

[27] X. Pan, A. H. Banihashemi, and A. Cuhadar, "Progressive transmission of images over fading channels using rate-compatible LDPC codes," *IEEE Trans. Image Process.*, vol. 15, no. 12, pp. 3627–3635, Dec. 2006.

[28] R. Puri, K. Ramchandran, K. W. Lee, and V. Bharghavan, "Forward error correction (FEC) codes based multiple description coding for internet video streaming and multicast," *Signal Process.: Image Commun.*, May 2001.

[29] D. G. Sachs, R. Anand, and K. Ramchandran, "Wireless image transmission using multiple-description based concatenated code," in *Proc. SPIE Image Video Commun. Process.*, 2000.

[30] A. Said and W. A. Pearlman, "A new fast and efficient image codec based on set partitioning in hierarchical trees," *IEEE Trans. Circuits Syst. Video Technol.*, vol. 6, no. 3, pp. 243–250, Jun. 1996.

[31] D. F. Shanno, "Conditioning of quasi-Newton methods for function minimization," *Math. Comput.*, vol. 24, pp. 647–656, 1970.

[32] J. M. Shapiro, "Embedded image coding using zerotrees of wavelet coefficients," *IEEE Trans. Signal Process.*, vol. 41, no. 12, pp. 3445–3462, Dec. 1993.

[33] P. G. Sherwood and K. Zeger, "Progressive image coding for noisy channels," *IEEE Signal Process. Lett.*, vol. 4, no. 7, pp. 189–191, Jul. 1997.

[34] M. K. Simon and M. S. Alouini, *Digital Communication Over Fading Channels: A Unified Approach to Performance Analysis*. New York: Wiley, 2000.

[35] B. S. Srinivas, R. Ladner, M. Azizoglu, and E. A. Riskin, "Progressive transmission of images using MAP detection over channels with memory," *IEEE Trans. Image Process.*, vol. 8, no. 4, pp. 462–475, Apr. 1999.

[36] V. Stankovic, R. Hamzaoui, and D. Saupe, "Fast algorithm for rate-based optimal error protection of embedded codes," *IEEE Trans. Commun.*, vol. 51, no. 12, pp. 1788–1798, Nov. 2003.

[37] V. Stankovic, R. Hamzaoui, and Z. Xiong, "Packet loss protection of embedded data with fast local search," in *Proc. IEEE ICIP*, 2002.

[38] V. Stankovic, R. Hamzaoui, and Z. Xiong, "Real-time error protection of embedded codes for packet erasure and fading channels," *IEEE Trans. Circuits Syst. Video Technol.*, vol. 14, no. 8, pp. 1064–1072, Aug. 2004.

[39] V. Tarokh, H. Jafarkhani, and A. R. Calderbank, "Space-time block coding for wireless communications: Performance results," *IEEE J. Sel. Areas Commun.*, vol. 17, no. 3, pp. 451–460, Mar. 1999.

[40] V. Tarokh, H. Jafarkhani, and A. R. Calderbank, "Space-time block coding from orthogonal designs," *IEEE Trans. Inform. Theory*, vol. 45, no. 5, pp. 1456–1467, Jul. 1999.

[41] D. Taubman and M. Marcellin, *JPEG2000: Image Compression Fundamentals, Standards, and Practice*. Norwell, MA: Kluwer, 2001.

[42] N. Thomos, N. V. Boulgouris, and M. G. Strintzis, "Optimized transmission of JPEG2000 streams over wireless channels," *IEEE Trans. Image Process.*, vol. 15, no. 1, pp. 54–67, Jan. 2006.

[43] S. Wicker, *Error Control Systems for Digital Communications and Storage*. Englewood Cliffs, NJ: Prentice-Hall, 1995.

[44] H. Yousefi'zadeh and H. Jafarkhani, "Statistical guarantee of QoS in communication networks with temporally correlated loss," in *Proc. IEEE GLOBECOM*, 2003.

[45] H. Yousefi'zadeh, H. Jafarkhani, and M. Moshfeghi, "Power optimization of wireless media systems with space-time block codes," *IEEE Trans. Image Process.*, vol. 13, no. 7, pp. 873–874, Jul. 2004.

Homayoun Yousefi'zadeh (SM'06) received the B.S. degree from Sharif University of Technology, Tehran, Iran, the M.S. degree from Amirkabir University of Technology, Iran, and the Ph.D. degree from University of Southern California, Los Angeles, all in electrical engineering, in 1989, 1993, and 1997, respectively.

He is currently with the faculty of the Department of Electrical Engineering and Computer Science at the University of California, Irvine. He also holds a consulting scientist position at the Boeing company. Most recently, he was the CTO of TierFleet, Inc., working on distributed database systems, a Senior Technical and Business Manager at Procom Technology, focusing on storage networking, and a Technical Consultant at NEC Electronics, designing and implementing distributed client-server systems.

Dr. Yousefi'zadeh has served as the chairperson of the systems' management workgroup of the Storage Networking Industry Association (SNIA), and a member of the scientific advisory board of the Integrated Media Services Center (IMSC) at the University of Southern of California. He is an associate editor for the IEEE Communications Letters, an editor of the IEEE Wireless Communications, and has been with the TPC of various IEEE conferences.

Hamid Jafarkhani (F'06) received the B.S. degree in electronics from Tehran University, Iran, in 1989 and the M.S. and Ph.D. degrees both in electrical engineering from the University of Maryland at College Park in 1994 and 1997, respectively.

In 1997, he was a Senior Technical Staff Member at AT&T Labs-Research and was later promoted to a Principle Technical Staff Member. He is currently a Professor at the Department of Electrical Engineering and Computer Science, University of California, Irvine, where he is also the Deputy Director of Center for Pervasive Communications and Computing.

Dr. Jafarkhani ranked first in the nationwide entrance examination of Iranian universities in 1984. He was a co-recipient of the American Division Award of the 1995 Texas Instruments DSP Solutions Challenge. He received the Best Paper Award of ISWC in 2002, the 2006 IEEE Marconi Best Paper Award in Wireless Communications, and an NSF Career Award. He also received the UCI Distinguished Mid-Career Faculty Award for Research in 2006 and the School of Engineering Fariborz Maseeh Best Faculty Research Award in 2007. He was an Associate Editor for IEEE Communications Letters from 2001-2005, an editor for the IEEE TRANSACTIONS ON WIRELESS COMMUNICATIONS from 2002 to 2007 and an editor for the IEEE TRANSACTIONS ON COMMUNICATIONS from 2005 to 2007. Currently, he is an area editor for the IEEE TRANSACTIONS ON WIRELESS COMMUNICATIONS. He is listed as a highly cited researcher in http://www.isihighlycited.com. He is author of the book *Space-Time Coding: Theory and Practice*.

Farzad Etemadi received the B.Sc. degree from Sharif University of Technology, Tehran, Iran, in 1991, and the M.Sc. and Ph.D. degrees from the University of California, Irvine, in 1998 and 2007, respectively, all in electrical engineering.

From 1992 to 1995, he was a Research Engineer at the Electric Power Research Center, Tehran. He worked on digital ASIC design at Standard Micorosystems Corporation (SMC), Irvine, in the summer of 1997. From 1998 to 2002, he worked as an ASIC Design Engineer for cable/digital TV, cable modem and satellite applications at the Broadband Communications Group of Broadcom Corporation, Irvine. In 2007, he returned to Broadcom, where he is currently working on the system design for cellular and Bluetooth applications in the Wireless Connectivity Group. His current research interests include multimedia communications, joint source-channel coding, and information theory.